

**RERTR 2009 – 31<sup>st</sup> INTERNATIONAL MEETING ON  
REDUCED ENRICHMENT FOR RESEARCH AND TEST REACTORS**

November 1-5, 2009  
Kempinski Hotel Beijing Lufthansa Center  
Beijing, China

**STUDY ON IN-PILE PERFORMANCE OF SILICIDE FUEL  
UNDER POWER TRANSIENT**

KAZUAKI YANAGISAWA  
Policy Planning and Administration Department  
Japan Atomic Energy Agency  
1233 Watanuki, Takasaki, Gunma, 370-1292, Japan

**ABSTRACT**

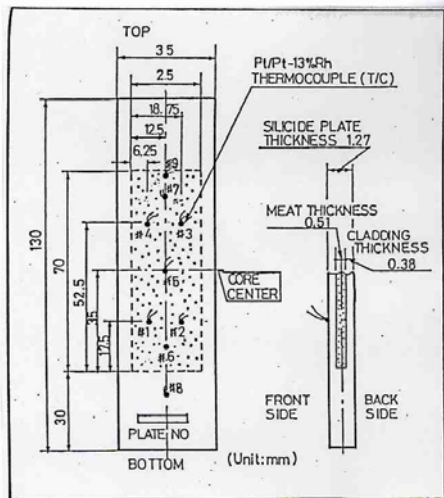
Power transient test was conducted on un-irradiated silicide mini-plate fuels. A failure threshold of tested fuel is revealed between 82 and 94 cal/g·fuel plate. Failure mechanism of a through-plate cracking is a thermal stress caused by a large temperature drop ( $\Delta T > 94$  deg.C), combined with a rapid quench ( $< 0.13$ s). Additionally, a water channel closure (plate bowing) was studied by triplet and single plate configurations as a function of peak cladding surface temperature (PCST). From this study adaptability of licensing criteria (228 deg.C) applied to the water channel closure of Japan Research Reactor-3 (JRR-3) and Japan Materials Testing Reactor (JMTR) silicide fuels are experimentally confirmed.

**1. Introduction**

To understand a power transient behaviour of a low enriched uranium silicide mini-plate fuel for material testing and research reactors, the experiment was conducted on un-irradiated mini-plate fuels at Nuclear Safety Research Reactor (NSRR) in JAEA (The former Japan Atomic Energy Research Institute, JAERI). In experiments, a fuel failure threshold and a failure mechanism as well as a water channel closure (plate bowing) were studied by means of in-core instrumentations and post-pulse irradiation examination (PIE). The results obtained in this study should be useful as a database for safety evaluation of water-cooled research reactors used in the world [1].

## 2. Experiment

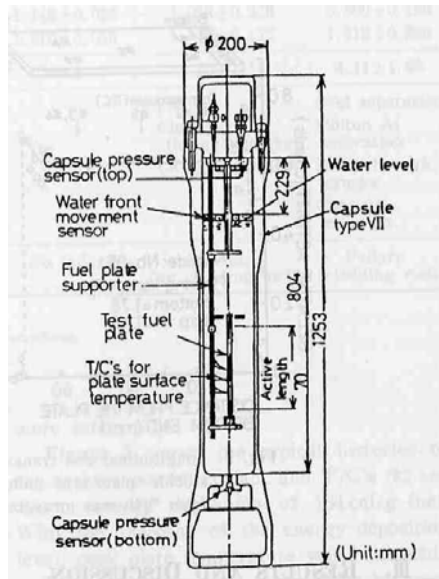
### 2.a Test Mini-Plate Fuel



The test mini-plate fuels used in this study were designed by JAERI and fabricated by two foreign vendors; CERCA in Romans, France and B&W in Lynchburg, Virginia., the U. S. The outline of it is schematically shown in **Fig. 1**. Similar plate-type fuels are fabricated for the cores of JMTR and those of JRR-3. The fabrication processes for these mini-plate fuels were described elsewhere [2, 3]. The test mini-plate fuel consists of the fuel core (25×70×0.51mm) sandwiched by Al-3wt%Mg based alloy cladding (35×130×0.38mm), hereinafter abbreviated as “Al cladding”.

*Fig. 1: Schematic presentation of tested silicide mini-plate fuel having enrichment by 19.89 wt%  $^{235}\text{U}$  and density by 4.8 gU /c.c.*

## 2.b Instrumentation and Irradiation Capsule



The in-core instrumentation was Pt/Pt-13%Rh bare wire thermocouples (0.2mm outer diameter), hereinafter abbreviated as “T/C’s”. Of which melting point was 1,780 deg.C. These were, as shown in Fig. 1, spot welded directly to the external surface of the mini-plate fuel at different locations. The maximum numbers of welded T/C’s a mini-plate fuel were nine. In most experiments, however, T/C’s used were five. After assembling mini-plate fuel in the supporting jig with electric cables, it was loaded into irradiation capsules as shown schematically in **Fig. 2**. All the irradiation tests with those instrumentations were conducted in stagnant water at room temperature about 20 deg.C and one atmospheric pressure inside the sealed irradiation capsule [4].

Fig. 2: Schematic drawing of NSRR irradiation capsule for experimental series of 508, designed for the in-core tests of silicide mini-plate fuels.

## 2.c Pulse history

The half-width of power of NSRR pulse irradiation is a minimum of about 4.4ms at a maximum integral power of 110MW·s. The value of this width varies from 4.4 to 20ms depending on the magnitude of inserted reactivity. The effect of pulse width variation in this experiment is, however, negligible since the pulse-width is far below the thermal time constant of the mini-plate fuel (approximately 0.1s). The integral value of the reactor power  $P$  (MW·s) measured by micro fission chambers was used to estimate deposited energy  $E_g$  (cal/g·fuel plate) in each test mini-plate fuel. Hence,  $E_g = kg \times P$ , where the power conversion ratio  $kg$  (cal/g·fuel plate per MW·s), is the ratio of mini-plate fuel power to reactor power. This ratio was determined through a fuel burn-up analysis [5], taking the radial and axial power skew into consideration.

## 3. Results and Discussion

### 3.a Transient Temperature

In **Fig. 3**, a typical transient temperature measured by T/C #4 that received an energy deposition of 97 cal/g·fuel plate is shown with the pulse power, indicated by dotted line. It can be seen from the figure that cladding surface temperature (hereinafter abbreviated as CST) exceeded the boiling temperature,  $T_i$  (154 deg.C), beyond the saturation temperature,  $T_{sat}$  (100 deg.C), due to the pulse irradiation. Commencement of coolant boiling at temperature  $T_i$  was determined by data from the capsule water level sensor. Namely, the timing of coolant boiling was detected by the movement of water free surfaces, and the timing of water free surface movement is detected by the floating buoy having a magnetic sensor inside. The CST continued to increase to an overshoot temperature,  $T_{ov}$  (203 deg.C). It then decreased to 194 deg.C and remained <10ms. This CST was thought to be the commencement of film boiling. The author signify it as  $T_{DNB}$  and denote here as the departure from nucleate boiling (DNB) temperature. A signal of DNB temperature can be detected from a temperature plateau, which should be appeared after  $T_{ov}$ .

The DNB value was found to be  $174 \pm 6$  deg.C from the average of 31 data points. Above  $T_{DNB}$ , the increase in CST terminated at temperature  $T_{max}$  (244 deg.C). The CST was then quenched to temperature  $T_p$  (116 deg.C) during an interval of  $t_p$  (0.135s). The magnitude of the temperature difference is given by  $\Delta T = T_{max} - T_p$  and is denoted here as the “temperature drop (128 deg.C for this case)”. Note that peak CSTs (hereinafter abbreviated as PCST) measured in the course of experiments are above  $T_{DNB}$  except one which is performed intentionally to have  $PCST < T_{DNB}$  (experiment 508-12, 32 cal/g · fuel plate).

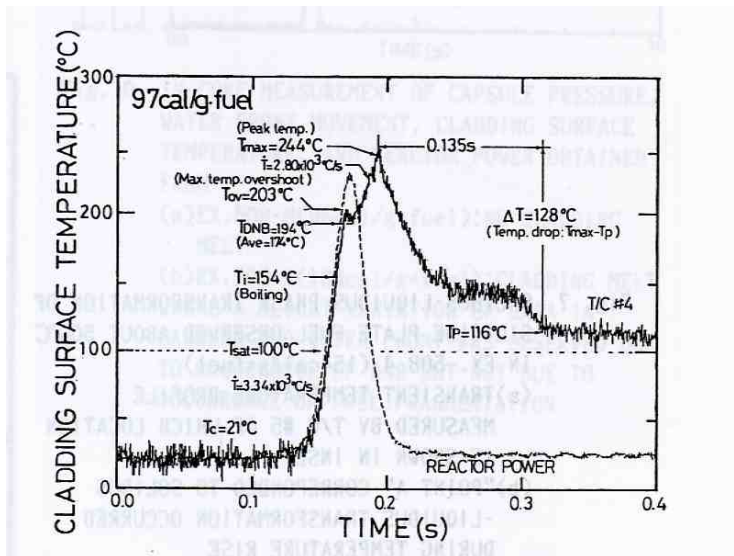


Fig. 3: Typical example of cladding surface temperature (solid line) and reactor power (dotted line), showing boiling temperature ( $T_i$ ), DNB temperature ( $T_{DNB}$ ), maximum overshoot temperature ( $T_{ov}$ ), peak cladding surface temperature ( $T_{max}$ ), quench temperature ( $T_p$ ), temperature drop ( $\Delta T$ ), and time to quench ( $t_p$ ). These are from T/C #4 of the mini-plate fuel used in experiment 508-8 (97 cal/g · fuel plate, failure).

### 3.b Failure Threshold

Fig. 4 summarizes the relation between the measured PCST and the given deposited energy. Note again that all PCST are above  $T_{DNB}$  except one case (32 cal/g · fuel plate). The tested mini-plate fuels are intact at energy depositions  $< 82$  cal/g · fuel plate, while they are damaged at energy deposition  $> 94$  cal/g · fuel plate except one mini-plate pulsed at 98 cal/g · fuel plate without T/C's. The cause of this exception is not clear.

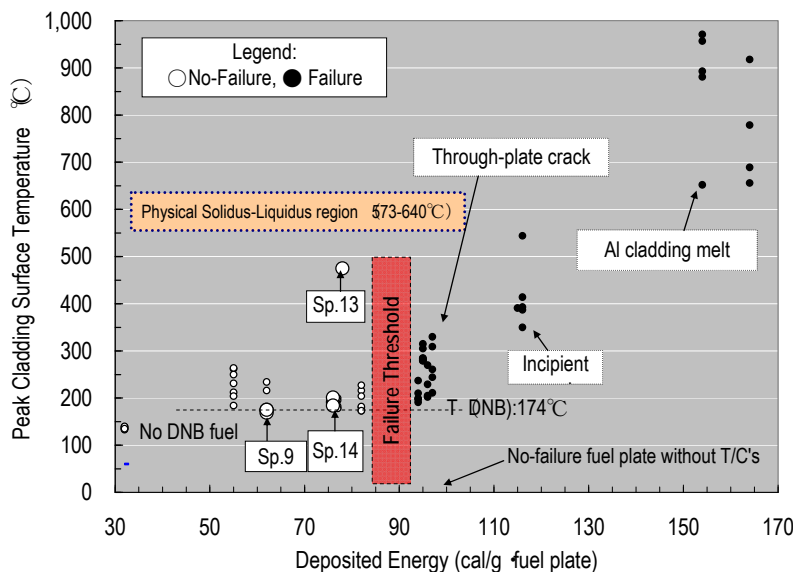


Fig. 4: PCST read directly from the spot welded T/C as a function of deposited energy, where data point from experiment with no T/C is shown by arrow at the corresponded energy deposition. The dotted line indicates the  $T_{DNB}$  (174 deg.C). Three specimens; Sp.9, Sp.13 and

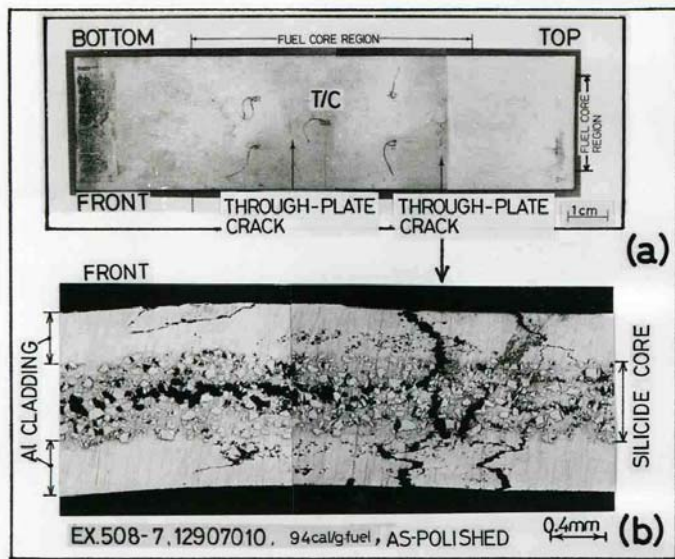
Sp.14 is provided for test in triplet rod configuration. Due to mechanical blockage to prevent coolant cross flow, Sp.13 had a significant PCST up to 475 deg.C but did not fail.

### 3.c Failure Mechanism

The failure mode was significantly dependent on deposited energy that is, directly related to PCST. It is revealed from the figure that there are two failure modes. One is either a through-plate cracking (<400 deg.C) or an incipient cracking occurred between 400 deg.C and 640 deg.C. The other is apparently Al cladding melt. Detail discussion about failure mode is as follows;

#### (1-1) Through-plate cracking failure

For through-plate cracking, a typical example is shown in **Photo. 1** (94 cal/g·fuel plate, PCST: 237deg.C). Two major through-plate cracks propagated perpendicularly from a cladding external surface to fuel core. These cracks are intergranular and rather tight, and they existed locally. This



occurred without accompanying significant dimensional changes to the tested mini-plate fuel. The observed damage is likely to be a hardening crack led by a thermal stress due to the temperature drop  $\Delta T$ . The calculated thermal stress caused by  $\Delta T$  is ranged between 156 and 216MPa, which is greater than the tensile stress (120MPa) and 0.2% proof strength (85MPa) of the tested mini-plates. It implies that the local stress arising from the temperature drop  $\Delta T$  during the quench is enough to affect on test mini-plate fuel cracking.

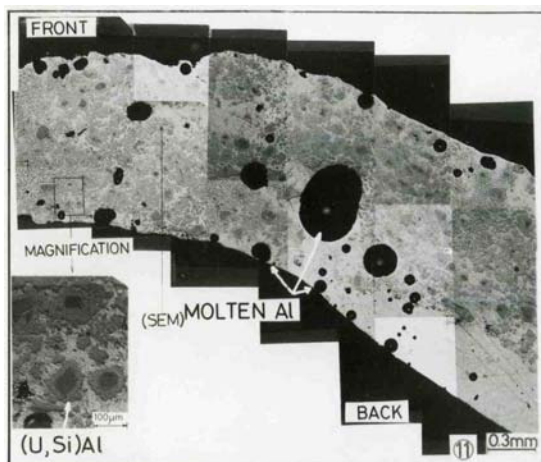
Photo 1: (a) Overview of the test mini-plate fuel at 94 cal/g · fuel plate

(PCST: 237 deg.C), where two through-plate cracks observed locally.(b)The polished longitudinal section cut from the through-plate crack at the plate top region.

#### (1-2) Incipient cracking failure

At temperatures between 400 and 640 deg.C, the test mini-plate fuels failed by incipient cracking, accompanied by a significant plate deformation. This seems to be influenced by annealing of Al cladding. Namely, crack propagation from Al cladding surface during quench might be ceased at annealed (softened) Al material.

#### (2) Al cladding melt



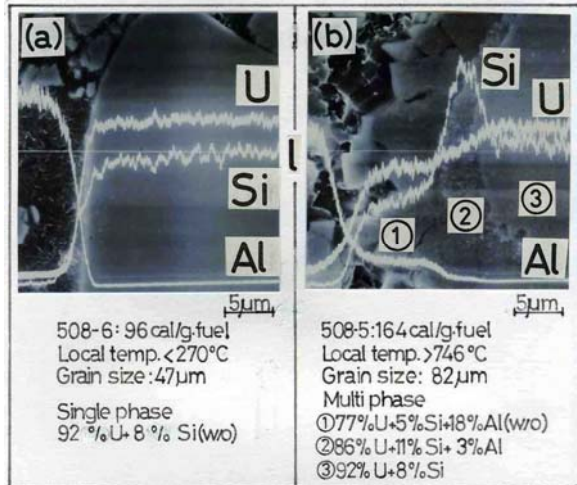
At temperature beyond the Al cladding melt (>640 deg.C), the test mini-plate fuel failed accompanied with significant formation of molten Al holes, molten Al agglomeration (see, **Photo 2**), fuel core separation, and through-plate cracking.

Photo 2: Cross section of pulsed mini-plate fuel at energy deposition 164 cal/g · fuel plate, where PCST was about 918 deg.C. Formation of molten Al holes and molten Al agglomeration are observed.

### (3) Destructive Force

In-core data for no cladding melt condition and that for cladding melt condition are compared each other. In both cases, neither a detectable increase of capsule pressure nor a movement of water column was observed. Hence, in spite of drastic damage, the test mini-plate fuel did show neither fragmentation nor destructive force that would be expected to occur by interaction of molten fuel with coolant [6].

### (4) PIE



In **Photo 3**, SEM/XMA (scanning electron microscope combined with x-ray micro analyzer) for (a) PCST<270 deg.C and (b) PCST>746 deg.C are shown. In the former, a microstructure composed of fuel elements U, Si and Al did not change significantly. In the latter, however, a reaction between aluminium matrix and silicide particle did occur due to the diffusion of the composed elements. As a result, two additional new phases at outermost of the silicide particles were formed.

*Photo 3: SEM/XMA examined along line l shown in the central part of the picture, where (a) the specimen had 96 cal/g ·fuel plate with PCST<270 deg.C and (b) the specimen had 164 cal/g ·fuel plate with PCST>746 deg.C. A relative magnitude of detected elements was Al : Si :U =1 : 1: 5 for (a) and Al : Si :U =1 : 2.5: 5 for (b).*

### 3.d Water channel closure by single plate configuration

(For technical terminology, hereinafter, the author wishes to use “bow” as a cause of the phenomenon and “water channel closure” as a result of the phenomenon.)

JRR-3 safety analyses principally performed by the EUREKA-2 computer code [7] predicted that the licensing limit of the water channel closure was about 228 deg.C for silicide fuel. To verify this matter from the experimental point of view, a plate bow was studied from PIE. Hence, the magnitude of bow was determined by specimens cut longitudinally or transversally from a pulsed mini-plate fuel. A plate cut was made along to the T/C to make correspondence between the bow and PCST. In **Fig. 5**, the bowing of the silicide mini-plate fuel is shown. Up to the mini-plate fuel temperature of 400 deg.C, the bowing was less than 1mm (42% gap closure in maximum case), still remaining a safety margin for the coolant flow. When the temperature was exceeded 400 deg.C, however, a bowing tended to close the water gap. The bow was significant by occurrence of a marked thinning of the plate wall thickness at the end peak locations.

Strictly speaking, the bow determined by a single plate configuration may not sufficient for evaluating the safety margin of water channel closure because in conventional research reactor many fuel plates are in the form of assembly. To simulate more practical condition, an irradiation test by triplet plate configuration is planned. Results are shown in the subsequent section.

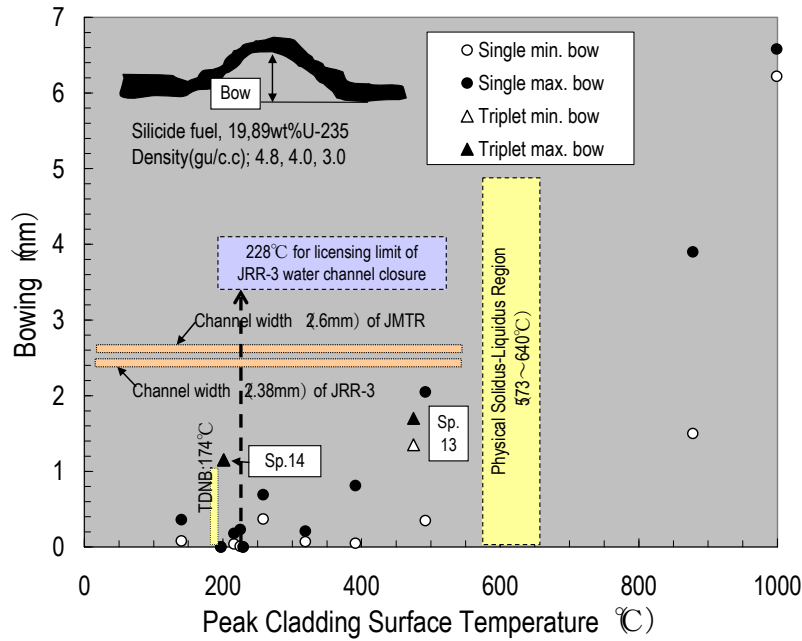
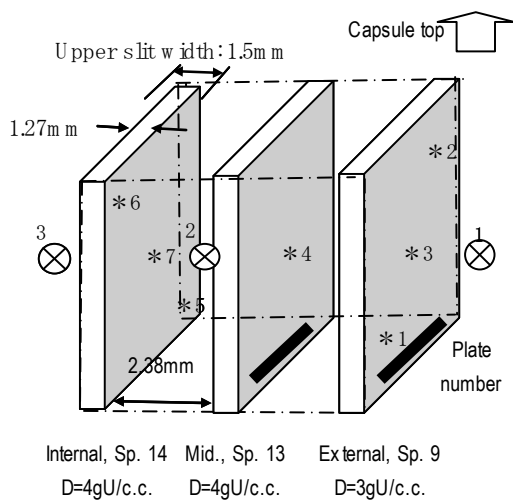


Fig. 5: Observed maximum and minimum bowing of silicide mini-plate fuel at PIE; where cuttings a plate were made either of longitudinal section (T/C #5) or of transversal sections (all T/C's except #5) in order to contain at least one T/C in a cut specimen . Circles are from single plate configuration and triangles are from triplet plate configuration. As for reference, channel width of JMTR (2.6mm) and that of JRR-3 (2.38mm) are drawn as horizontal bars. Furthermore, a temperature (228 deg.C) of licensing limit of JRR-3 for a water channel closure is indicated by vertical broken line together with  $T_{DNB}$  (174 deg.C) point

### 3.e Water channel closure by triplet plate configuration



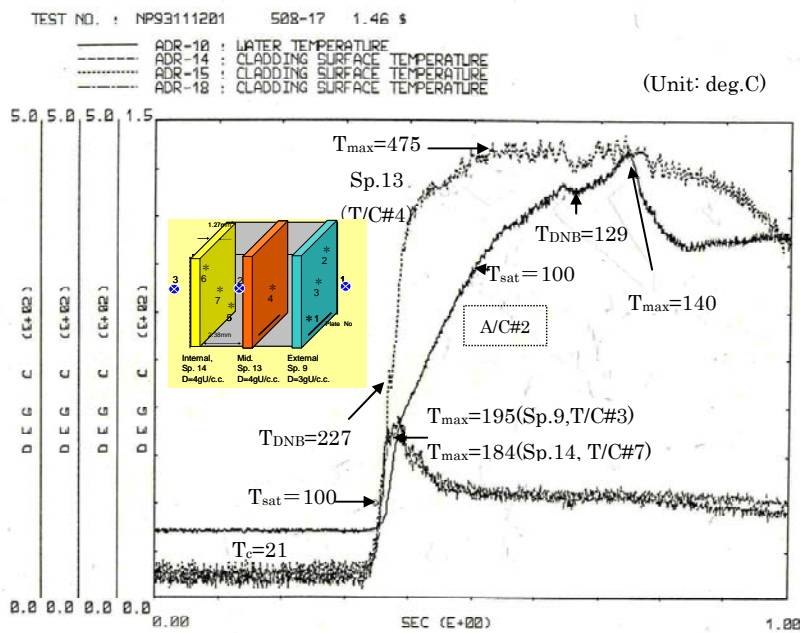
Channel gap: 2.38mm, Fuel plate thickness: 1.27mm  
 \* PVPt-13%Rh bare wire thermocouple(T/C)  
 ⊗ Water thermocouple (A/C) distanced 1mm from a fuel plate surface  
 To block coolant cross flow, both sides of fuel plate are mechanically blocked by two aluminum plates ( - - )

As shown in Fig.6, silicide mini-plate fuels (4.0 and 3.0gU/c.c.) fabricated by a scale factor of 1/5 of JRR-3 were arranged with a triplet configuration to have a water gap by 2.38mm. At top of each specimen, one set the upper slit having width by 1.5mm. To give a significant temperature rise in Sp.13, both longitudinal sides of the test specimens are mechanically blocked by the aluminium plates, as shown in dotted chain lines in the figure. Due to this, a coolant cross flow of Sp.13 is intentionally blocked. After pulse irradiation to 78cal/g·fuel plate, a water channel closure of triplet plate configuration was studied. Major observations are described in the followings.

Fig. 6: Schematic drawing of triplet mini-plate fuel configuration.

(1) Behaviour of temperature

In Fig. 7, transient temperature from the coolant(A/C#2) is plotted as a function of time (1s). It shows that the coolant temperature in the water gap increased rapidly from 21 deg.C through the saturation temperature  $T_{sat}$  (100 deg.C) to the DNB temperature  $T_{DNB}$  (129 deg.C) due to transient.  $T_{DNB}$  defined previously, is thought to indicate the commencement of the film boiling.



The coolant temperature increased above DNB, peaked at  $T_{max}$  (140 deg.C) and then began to decrease due to quenching. On the other hand, coolant temperatures measured by A/C#1 and A/C#3 increased only to a maximum of about 50 deg.C. Thus, a significant vaporization of the coolant occurred only in the water gap locations. The signal from the water level sensor fluctuated little, meaning that no mechanical energy was released from any of the tested specimens.

Fig.7: Coolant temperature monitored by A/C#2 at the water channel gap and PCST monitored by T/C#4 at the centre location of specimen 13 as a function of time (1s).

On the other hand, CST of Sp.13 increased from  $T_c$  (21 deg.C) through the saturation temperature  $T_{sat}$  (100 deg.C) to  $T_{DNB}$  (227 deg.C). Above  $T_{DNB}$ , the increase in the CST peaked at temperature  $T_{max}$  (475 deg.C) or PCST. The rate of temperature rise was roughly  $7.5 \times 10^3$  K/s. The PCST in the other two specimens was relatively low; 195 deg.C for Sp.9 and 184 deg.C for Sp.14.

From data plotting for the first 10s it is revealed that the CST of Sp.13 was dropped from  $T_{max}$  (475 deg.C) to  $T_p$  (121 deg.C) during 0.91s, while CST of Sp.9 and Sp.14 were dropped to  $T_{max}$  to  $T_p$  during 0.07s. The temperature drop  $\Delta T$  was 354 deg.C for Sp.13, 60 deg.C for Sp.9 and 73 deg.C for Sp.14.

Despite of a significant PCST under evaporated coolant condition, Sp.13 did not fail. The author focused on this point. Data from previous experiments [6] are plotted together in Fig. 8. The author revealed that fuel failure is led by a large local tensile stress at an energy deposition  $>94 \text{ cal/g} \cdot \text{fuel plate}$ . In that case, two parameters seem to be important. One is rapid quenching ( $<0.13\text{s}$ ) and the other is large  $\Delta T$  ( $T_{max} - T_p$ )  $> 94$  deg.C. This is clear by comparison between Sp.13 (intact) and CS514819 (failure), shown in the figure. Even though

the former had a high PCST (475deg.C) and a large  $\Delta T$  (350deg.C), it did not fail because of longer time to quench (0.91s). The value was about 7 times longer than that of the latter (0.129s). Consequently, the time to quench seems to be important factor for through-plate cracking.

Sp.9 and Sp.14 had a potential to cause fuel failure due to the shorter values in time to quench. However, they did not fail because of the smaller values in  $\Delta T$ ; that is 60 deg.C for Sp.9 and 73 deg.C for Sp.14. It is interesting to say that they were as close as the failure point represented by Sp.12907010.

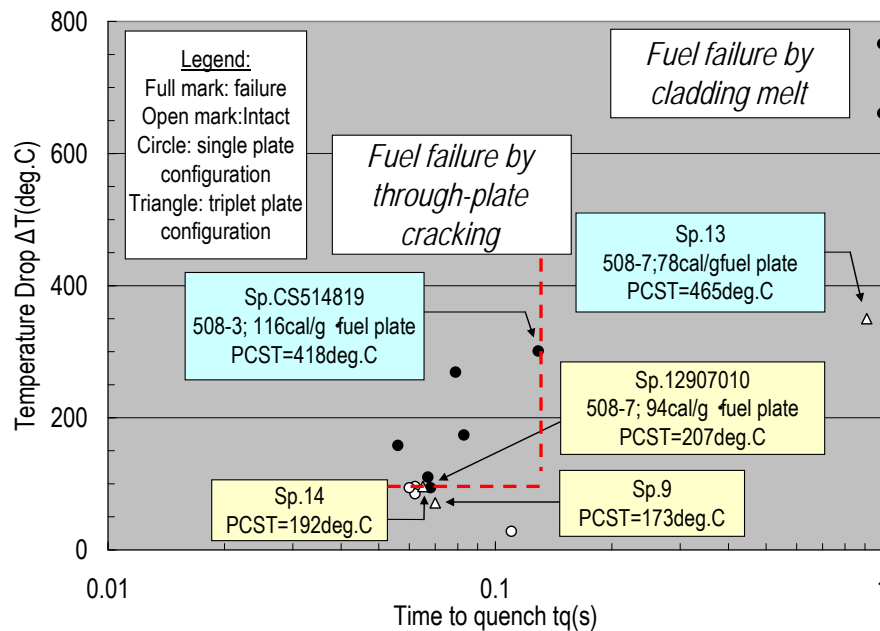
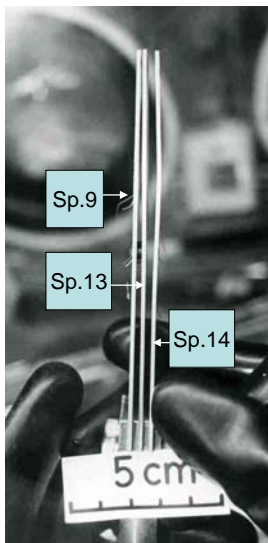


Fig. 8: Temperature drop  $\Delta T$  as a function of time to quench  $t_q$ . Sp.13 had a potential to cause failure due to large  $\Delta T$  but did not fail due to a relative long time to quench (0.91s). Sp.9 and Sp.14 did not fail due to have a small magnitude in temperature drop.

## (2) Bow



The irradiation capsule was unloaded from the NSRR core to observe the bow of tested specimens. Note that they had straightness before irradiation. After the removal of two aluminium plates set for blockage of cross flow, apparently Sp.14 bowed towards the open gap side, where the PCST is  $192 \pm 9$  deg.C and coolant temperature at open gap was 49 deg.C. The maximum bow was about 1.15mm occurred in the vicinity of T/C #6. This bow can be explained by "bimetal effect under slit restriction". Hence, after pulse, Sp.14 was heated up to 192 deg.C. A coolant was simultaneously heated up to 140 deg.C at water gap and 49 deg.C at open gap. Because of unbalanced temperature profiles Sp.14 tended to bow towards water gap due to a bimetal effect. This movement, however, was restricted by the existing top slit. Because as-fabricated gap was 2.38mm, the resultant closure of water gap was about 48% (1.15mm).

*Photo 4: After removal of top slit, Sp.13 bowed gradually towards direction to Sp.9. A magnitude of gap closure between Sp.13 and Sp.9 is 71% (1.7mm) in maximum.*

To my surprise, Sp.13 did not bow at this instance, though it had high PCST (475 deg.C) and high coolant temperature (140 deg.C) at both water gap sides. After dismantling the top slit from the supporting jig, Sp.13 bowed towards Sp.9. This condition is shown in the **Photo. 4**. Bow measured by a clearance gauge was about 1.35-1.45mm and bow measured by magnified photograph was 1.7mm. The latter is used as the maximum bow; a corresponded water channel closure was 71%. Bow in Sp.13 might be enhanced by an annealing of Al-cladding occurred at a half of melting point. Resultantly it left the local residual stress behind because of distorted annealing temperature profiles.

Sp.9 did not bow at all. The PCST was  $173\pm 3$  deg.C and coolant was 51 deg.C at the open gap side (no A/C was set at the water gap side). Relative low PCST compared with Sp.14 may be the reason of no bowing. Due to the different fuel density, heat up rate is 7 deg.C/1000s for the former and 54 deg.C/1000s for the latter. Temperature drop  $\Delta T$  is 96 deg.C for the former and 71 deg.C for the latter, respectively.

Subsequently, one dismantled a bottom end clamp to examine the surface conditions of the tested specimens. Sp.13 had no anomalies except backside, where the surface was discoloured over a range about 17mm. This might be caused by a turbulence of coolant at A/C #2 located in the vicinity of the area. The Sp.14 also had a very smooth surface showing no anomalies except at the top edge, where a trace of mechanical interaction between the specimen and the slit was observed. The interaction might have resulted from the bow of the specimen. At PIE, no fuel failure was observed to all three specimens.

The bow of Sp.13 and Sp.14 are plotted together with previous data and included in Fig. 5. Sp.9 was omitted due to no bow. Despite of a mechanical blockage, the magnitude of bow of the two specimens are as the same level as those obtained from single plate configuration. This implies that the bow data from single plate configuration is also useful as licensing data points. For water channel closure of JRR-3, the licensing upper point defined by EUREKA-2 computer code is 228 deg.C. It is indicated by the vertical broken line in the figure. Because all experimental data below 228 deg.C are less than 2.38mm (channel width of JRR-3), experimental results substitute the safety margin of EURECA prediction. A worst case is of course Sp.14.

From a fuel microstructure, it is found that fuel particles did not form a secondary metal phase because of a temperature ( $< 475$  deg.C). No anomalies are observed in all tested specimens.

#### **4. Conclusions**

The conclusions reached in the present study are summarized as follows:

- (1) The tested silicide mini-plate fuels were intact at energy depositions  $< 82$  cal/g·fuel plate but were damaged at energy deposition  $> 94$  cal/g·fuel plate. A failure threshold must exist between these two values. The departure from nucleate boiling about 174 deg.C and the temperature drop  $\Delta T > 72$  deg.C during quenching occurred in all tested fuel plated at energy depositions  $> 62$  cal/g·fuel plate.
- (2) The failure mechanism was dependent on the energy deposition, in turn was strongly associated with the PCST of the tested fuel plate. Failure at temperature below 640 deg.C (Al melting point) is caused by the thermal stress induced by the temperature drop ( $\Delta T > 94$  deg.C) combined with a rapid quench ( $< 0.13$ s). Several local

intergranular cracks perpendicular to the axial direction of the plate have propagated from the cladding external surface to the fuel core. Test mini-plate under this situation showed little dimensional changes. Failure at temperature above 640 deg.C is caused by the Al cladding melt. Test mini-plate under this situation showed large dimensional changes

- (3) Within this experimental scope (temperature <970 deg.C), no destructive force as a result of interaction between molten Al and coolant was observed.
- (4) During test with triplet configuration, Sp.13 had mechanical blockages to prevent coolant cross flow. The PCST of Sp.13 at 78cal/g·fuel was 475deg.C and coolant temperature at the water gap was 140 deg.C. Due principally to the long quench (0.91s from 475deg.C to 121deg.C), no mechanical failure occurred. The maximum bow was 1.7mm, that is, about 71% closure of water gap.
- (5) Adaptability of a licensing criteria (228 deg.C) applied to the water channel closure of JRR-3 and JMTR silicide fuels are experimentally confirmed.

### Acknowledgments

Grateful thanks are addressed to Dr. Toshio Fujishiro, the former Director, the Department of Nuclear Safety Research, Japan Atomic Energy Research Institute (JAERI) for his useful suggestions in the course of the present study. Acknowledgment is also addressed to Ms. Yuko Nakajima, belonged to the Office Automation Systems Management and Operating Office, Centre for Computational Sciences' & e-Systems, Japan Atomic Energy Agency (JAEA), for her excellent editing to the whole text structures and arrangement of tables and figures.

### References

- [1] F. Yoshino and R. Kimura, "Outline of Examination Guides of Water-Cooled Research Reactors", JAERI-M 92-028, (1992).
- [2] USNRC, "Safety Evaluation Report Related to the Evaluation of Low-Enriched Uranium Silicide-Aluminum Dispersion Fuel Use in Non-Power Reactors", NUREG-1313, (1988).
- [3] Y. Fanjas, "MTR fuel inspection at CERCA", Proc. 3rd Asian Symposium on Research Reactor, p.399 (1991).
- [4] K. Yanagisawa, T. Fujishiro., O. Horiki., K. Soyama., H. Ichikawa and T. Kodaira, "Dimensional stability of low enriched uranium silicide plate-type fuel for research reactors at transient conditions", *J. Nucl. Sci., Technology*, **29**{3}, 233(1992).
- [5] ASTM (American Standard for Testing and Materials), "Standard test method for atom percent fission in Uranium and Plutonium fuel (Neodymium-148 method)", E 321-96 (2005).
- [6] K. Yanagisawa., "Transient Behaviour of Low Enriched Uranium Silicide Plate-Type Fuel for Research Reactors during Reactivity Initiated Accident", *International Journal of Nuclear Energy Science and Technology*, **4** [2], 97-110 (2008).
- [7] N. Ohnishi, T. Harami, H. Hirose, M. Uemura, "EURECA-2: A Computer Code for the Reactivity Accident Analysis in a Water Cooled Reactor", JAERI-M 84-074 (1984).